Raman Enhancement on Graphene: Adsorbed and Intercalated Molecular Species

Naeyoung Jung[†,§]* , Andrew C. Crowther,[†,§] Namdong Kim,[‡] Philip Kim,[‡] and Louis Brus[†]

[†]Department of Chemistry, [‡]Department of Physics, and Columbia University, New York, New York, 10027 United States. [§]These authors contributed equally to this work..

ABSTRACT Strong Raman scattering is observed from iodine anions adsorbed at *ca.* 3% coverage on single layer graphene. In addition, the Raman signal from just one bromine intercalation layer inside three and four layer thick graphenes is observed. We analyze and model the intramolecular electronic, charge-transfer, and multiple reflection electromagnetic mechanisms responsible for this unusual sensitivity. Graphene is an excellent Raman substrate for adsorbed species showing intramolecular electronic resonance, because graphene efficiently quenches interfering excited-state luminescence. The Raman sensitivity for adsorbed and intercalated molecular species is highest for single layer graphene and decreases with increasing thickness. These phenomena are compared with surface enhanced Raman spectroscopy field enhancement and "chemical" Raman processes in aggregated Ag particles and on flat, highly reflective metal surfaces. The Raman spectra of adsorbed bromine layers are not observed, despite significant charge transfer to graphene. Charge transfer from adsorbed bromine is about one-half of charge transfer from intercalated bromine. We attribute the large Raman signal for both adsorbed iodine and intercalated bromine species to intramolecular electronic resonance enhancement. The signal evolution with varying graphene thickness is explained by multiple reflection electromagnetic calculations.

KEYWORDS: graphene · surface enhanced Raman spectroscopy · SERS · intercalation · adsorption · interference · iodine · bromine

Graphene, a single atomic sheet of bulk graphite, shows extreme physical strength and high electron mobility resulting from extensive π electron conjugation and delocalization. Molecular intercalation into bulk graphite shifts the Fermi level of individual graphene-like sheets by charge-transfer doping; this process has been studied for many decades.[1] With single or few layer thick graphenes, there is the additional possibility of Fermi level shift from doping by adsorption on the top and bottom graphene layers, in addition to intercalation between layers. Graphene Raman scattering is a versatile characterization tool of high sensitivity and specificity. In a recent paper, we showed that Br_2 and I_2 charge-transfer chemical doping significantly downshifts the single sheet graphene Fermi level, as measured by the frequency change of the graphene Raman G (carbon−carbon stretch) band.[2] In three and four layer thick graphenes with adsorbed I_2, unequal doping of surface and interior layers is observed as multiple graphene G frequencies.

In general Raman scattering is too weak to a produce signal from monolayer samples. Yet, in addition to the well-known Raman scattering of single layer graphene vibrations, we now report observation of strong Raman scattering from adsorbed and intercalated anionic halogen species, at small fractions of a monolayer coverage. These Raman spectra are observed because both intramolecular electronic and multiple reflection electromagnetic Raman intensity enhancement effects occur on and in graphene samples. We model and quantify these enhancement mechanisms for molecular species adsorbed onto, and intercalated into, few layer thick graphenes (*N*L graphenes, where *N* is the number of layers). We compare absolute intensities to those of the electromagnetically enhanced graphene G Raman mode, as a function of *N*. We calculate a strong multiple reflection interference effect that decreases the adsorbed molecular Raman signal 55 times on bulk graphite, as compared to adsorption on single layer graphene. This model agrees well with the anionic halogen data which shows a factor of 30 decrease. We compare this graphene molecular Raman enhancement effect with the molecular surface enhanced Raman spectroscopy (SERS) seen in aggregated Ag nanoparticles[3] and the multiple reflection Raman effect seen for thin absorbing films on reflective metals.[4]

Molecular intercalation into bulk graphite creates stable stoichiometric compounds (graphite intercalation compounds, or GICs) in stages. Gaseous bromine in equilibrium with graphite creates a stage two

*Address correspondence to nj2153@columbia.edu.

Received for review August 31, 2010 and accepted October 06, 2010.

Published online October 14, 2010.
10.1021/nn102227u

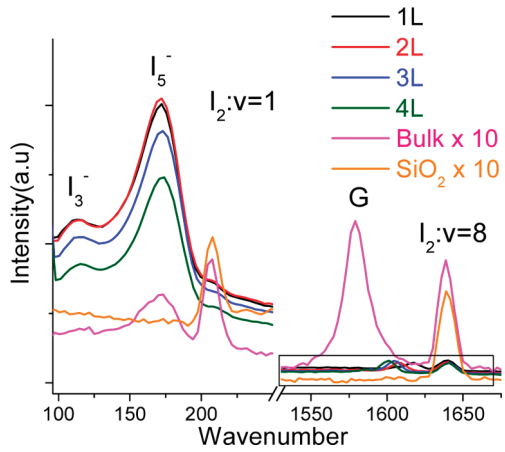

Figure 1. Raman signals of I_3^- and I_5^- stretching modes, and graphene G Raman signal, of 1−4L graphenes. Bulk Graphite and bare SiO_2 are shown, intensified 10 times for clear comparison. The line labeled $v = 1$ at *ca.* 210 cm^{-1} is the fluorescence of gas-phase I_2 above the graphene surface.

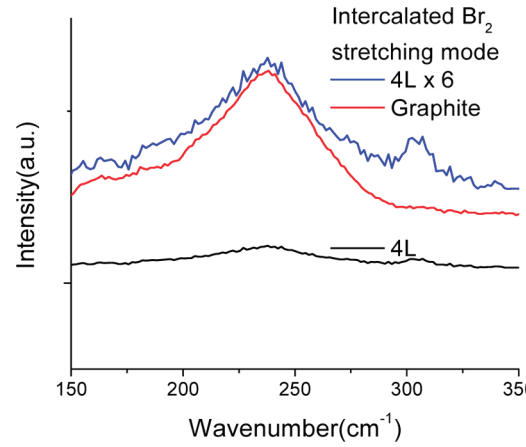

Figure 2. Raman signal of intercalated Br_2 in 4L graphene and graphite.

bulk GIC in which graphene bilayers (2L) are separated by intercalated Br_2 layers.[5−8] Such intercalated Br_2 layers are structurally commensurate with neighboring graphene.[5] The Raman spectrum shows the graphite G band up-shifted from 1580 cm^{-1} in pure graphite to 1612 cm^{-1} in the GIC, by a graphene electron transfer to bromine. The intercalated anionic Br_2 band near 240 cm^{-1}, downshifted from 323 cm^{-1} in free Br_2, is also observed.[6] In contrast, the Raman signal of adsorbed bromine on the top and the bottom of 1L graphene is not observed, even though such bromine does accept electrons from graphene as judged by the Raman G spectra.

Gaseous iodine does not form a corresponding GIC with graphite, apparently due to its longer (incommensurate) bond length compared with bromine.[9] Adsorbed I_2 accepts electrons from aromatic species, such as carbon nanotubes,[10−12] fullerenes,[13] pentacene films,[14,15] and polyacetylene,[16,17] and we observe that adsorbed iodine on graphene also accepts graphene electrons. The iodine anions thus created react with excess neutral I_2 to make I_3^- and I_5^- polyanions that absorb laser light strongly. There is a very strong, resonantly enhanced Raman signal at 108 and 165 cm^{-1} when visible laser wavelengths are employed. Note that the gas-phase Raman frequency of neutral I_2 is higher at 212 cm^{-1}.[18]

EXPERIMENTAL RESULTS

In Figure 1 the low-frequency Raman spectrum of I_2 exposed *N*L graphene samples shows intense Raman bands at 113 and 172 cm^{-1} which are assigned to the linear symmetric iodide anion I_3^- and linear symmetric I_5^- stretching bands.[18] These iodine anion transitions are far stronger than the allowed graphene G transition. The observed iodine surface anion Raman intensities decrease with increasing thickness in *N*L graphenes and become 30 times weaker on bulk graphite than on 1L graphene. Figure 2 shows the low-frequency Raman band of a single intercalated Br_2 layer in 4L graphene, comparing it with the intercalated Br_2 band in bulk graphite. As previously described, we observe Br_2 intercalation for $N = 3$ and larger graphenes. The single layer intercalated Br_2 Raman intensity in 4L graphene is six times smaller than the bulk graphite Br_2 Raman signal. We observe the Raman of intercalated bromine but not that of adsorbed bromine; yet both contribute to charge-transfer doping. We now try to understand all these observations.

Optical Interference and Raman Enhancement Calculations. ***Graphene G Mode.*** Two independent optical interference phenomena occur for graphene on the Si/SiO_2 substrate. First, in 1980 Connell, Nemanich, and Tsai showed that strong Raman scattering from thin absorbing films was obtained when the films were placed one-fourth of an optical wavelength in front of a highly reflective mirror.[19] For laser (and Raman) light propagating normal to the mirror, the reflected and incident traveling waves interfere to form a standing wave. Strong Raman scattering is observed when the film is spatially located at a standing wave constructive maximum. With graphene on the SiO_2(290 nm)/Si substrate, we have a modest back "mirror" effect of this sort; the back reflection coefficient of light in SiO_2 bouncing off Si is 21% at 632.8 nm laser wavelength. Second, the graphite metallic optical character for visible light (index of refraction $n = 2.88-1.75i$ at 632.8 nm)[20] creates a situation where multiple reflections of laser and Raman light occur as thickness changes in Figure 3. The multilayer graphene film acts internally as a modest optical cavity for both laser and Raman light, for example, G band Raman light (703 nm for He−Ne incident light) generated inside graphene has a near 38% back reflection probability at the graphene:air interface for normal incidence.

The Fresnel equations for multilayer optical interference have been known for many decades. With this approach Yoon *et al.*[21] calculated the single layer graphene G-peak intensity, and the 2D/G intensity ra-

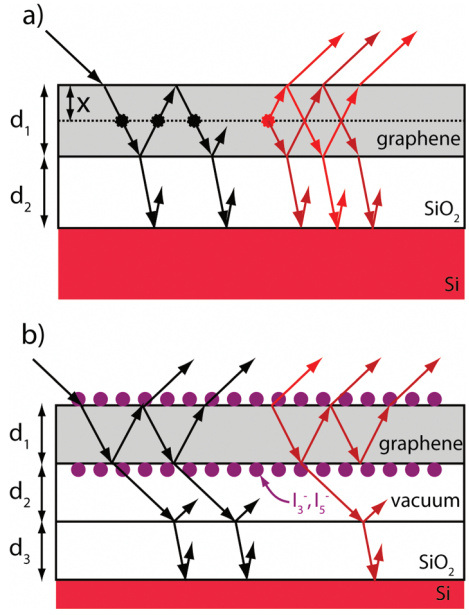

Figure 3. Schematic diagrams of multiple reflection interference (a) inside the graphene layers and (b) in the adsorbed molecules on the top graphene layer. The actual angle of incidence is 0° at normal incidence. (Black line represents the laser light electric field propagation direction, while red line represents Raman scattering light electric field propagation to the detector.)

tio, with varying SiO_2 thickness. Wang *et al.*[22] calculated the relative G intensity as a function of graphene thickness; however, their calculation did not allow the scattering light to shift phases during propagation, which affects Raman light self-interference. We now recalculate the graphene G intensity as a function of graphene thickness using the correct Raman self-interference model of Yoon *et al.*(equations in Supporting Information). We go on to calculate Raman intensities for both adsorbed and intercalated molecular species, as a function of graphene thickness, to understand our halogen anion data. For all calculations, the detected Raman peak energy gives the shift of the scattered wavelength relative to the incident wavelength.

At a given depth in graphene, the net laser intensity results from a sum over direct and reflected fields. The net Raman intensity also results from a sum over multiple Raman light pathways, including light initially scattered both toward and away from the detector as Figure 3a shows. The equation for the net detected Raman intensity is

$$I = |E\gamma|^2 = |F_{ab}E_0F_{sc}\gamma_0|^2 = |F_{ab}F_{sc}|^2|E_0\gamma_0|^2 \qquad (1)$$

where E_0 and γ_0 are the magnitude of the incident light field and the intrinsic Raman scattering cross section, and F_{ab} and F_{sc} are the net laser and Raman scattering enhancement factors constructed from Fresnel equations incorporating interference effects, following the notation of Yoon *et al.*[21]

The total G Raman intensity from all graphene layers, as a function of N, is obtained by first calculating

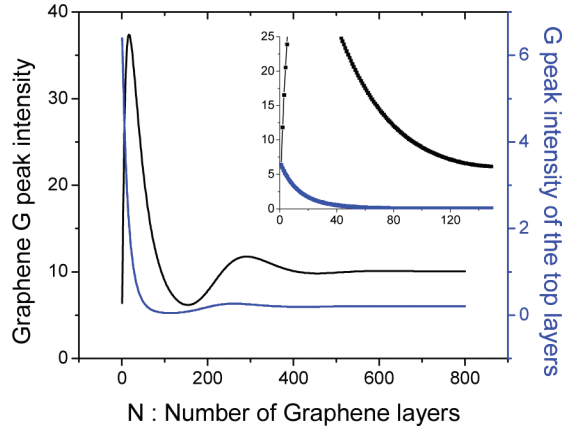

Figure 4. Black: Total graphene G peak intensity *versus* the number of layers as described in the text. Blue: G peak intensity of the top graphene layer *versus* the number of layers. The insert expands the image nearer the origin.

the net detected Raman light intensity generated at position x in graphene and then by integrating over the graphene thickness with the equation $I(N) = \int_0^{d_1(N)}|F_{ab}(x, N)F_{sc}(x, N)|^2dx$, where $d_1(N) = 0.335N$ is the graphene thickness in nanometers (0.335 nm is the thickness of one layer of graphene). In Figure 4 the total G Raman intensity rises to a peak at $N = 17$ and then shows a second smaller oscillatory peak near $N \sim 290$ in Figure 4. The $N = 1$ graphene G intensity of about two-thirds that of bulk graphite. The dependence on N is analogous to, but quantitatively different than, the theoretical result of Wang *et al.*[22] The $N = 17$ multilayer graphene shows a net G band intensity about 5.8 times larger than 1L graphene. This ratio matches the Wang *et al.* experimental data very well. Also shown is the G intensity of just the top graphene layer as a function of thickness; this top layer will have a different G frequency than interior layers if there is surface doping, as we observed previously for adsorbed iodine. The detected G intensity of the surface layer decreases with increasing thickness; for $N = 10$ the intensity is 52% of $N = 1$. Also note that for N values in this range, all interior graphene layers contribute equally to the total detected G Raman signal, assuming no surface doping (calculation not shown).

Iodine Adsorption. We now consider the detected Raman intensity of molecular species adsorbed on both the top and the bottom graphene surfaces. We neglect the change in the refractive index of the adsorbed layer as compared with vacuum; this is appropriate for low coverage. We set the graphene to SiO_2 distance to be 0.5 nm; the bottom adsorbed anion layer is in this space. The amplitude of the net laser field on top of the graphene in Figure 3b is the sum of the incident and the effective reflection fields from the lower interfaces: $E = E_0(1 + r_{04})$. The Raman signal for scattering dipoles just above the graphene (and oriented parallel to graphene) is $\gamma = \gamma_0(1 + r_{04})$, where $r_{04} = (r_{01} + r_{14}e^{-2i\beta_1})/(1 - r_{10}r_{14}e^{-2i\beta_1})$, $r_{14} = (r_{12} + r_{24}e^{-2i\beta_2})/(1 - r_{21}r_{24}e^{-2i\beta_2})$,

$r_{24} = (r_{23} + r_{34}e^{-2i\beta_3})/(1 - r_{32}r_{34}e^{-2i\beta_3})$ with $r_{xy} = (n_x - n_y)/(n_x + n_y)$ for $|x - y| = 1$ and $\beta_z = 2\pi n_z d_z/\lambda_0$. Thus, F_{ab} and F_{sc} both equal $|1 + r_{04}|^2$ for the top layer but with different wavelengths. The total Raman intensity of molecules above the graphene is

$$I = |E\gamma|^2 = |E_0\gamma_0|^2|1 + r_{04}|^4 \quad (2)$$

Applying the same methodology to the lower adsorbed layer gives

$$F_{ab} = \left|t_{02}\left(\frac{1 + r_{24}e^{-2i\beta_2}}{1 - r_{24}r_{20}e^{-2i\beta_2}}\right)\right| \quad \text{and} \quad F_{sc} = \left|t_{20}\left(\frac{1 + r_{24}e^{-2i\beta_2}}{1 - r_{24}r_{20}e^{-2i\beta_2}}\right)\right| \quad (3)$$

and a Raman intensity of:

$$I = |E_0\gamma_0|^2\left|t_{02}t_{20}\left(\frac{1 + r_{24}e^{-2i\beta_2}}{1 - r_{24}r_{20}e^{-2i\beta_2}}\right)^2\right|^2 \quad (4)$$

where $t_{02} = (t_{01}t_{12}e^{-i\beta_1})/(1 - r_{10}r_{12}e^{-2i\beta_1})$; $t_{01} = 2n_0/(n_0 + n_1)$; $t_{12} = 2n_1/(n_1 + n_2)$; and t_{20} follows the same pattern.

Figure 5 shows the calculated Raman intensities of the adsorbed molecules as a function of thickness. The detected Raman intensity is 1.3, with respect to the same species in vacuum at the same laser intensity, both above and below 1L graphene. This intensity decreases with increasing *N*. This behavior is quite similar to the decreasing G band intensity for the surface graphene layer in Figure 4. The calculated relative Raman enhancement on top of large *N* bulk graphite is quite low: 0.05; it is 0 on the bottom graphene surface as the laser does not penetrate through thick graphene.

Figure 6 shows a calculation of the reflected laser light, both with the back Si mirror and with the Si replaced with SiO_2, as would be appropriate for graphene on a quartz substrate. With the mirror, the net reflectivity for 1L graphene on the substrate is 15%. The net reflectivity actually decreases with increasing graphene thickness, showing a 4% minimum at *N* about 19. This behavior represents destructive interference of laser light reflected from the back Si mirror and from graphene; such destructive interference was discussed by Connell *et al.*[19] Without the mirror, the initial reflectivity of 1L graphene on the SiO_2 substrate is about 4%; this reflectivity grows linearly with increasing *N* initially. It shows a broad resonance near $N = 140$ before approaching the 36% bulk graphite reflection for large *N*.

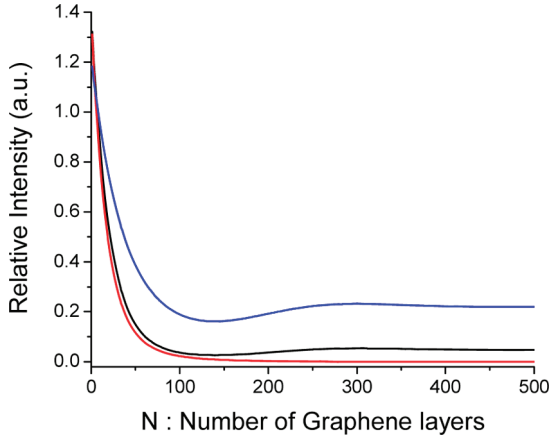

Figure 5. Blue: Laser intensity enhancement factor right above top graphene interface (relative to the free space). Black: Raman enhancement magnitude for adsorbed species on top graphene surface. Red: Raman enhancement magnitude for adsorbed species under graphene.

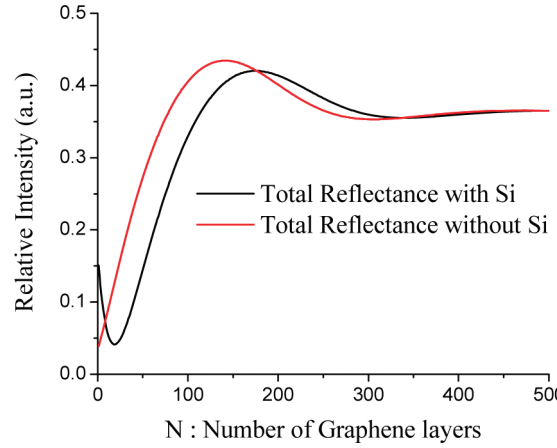

Figure 6. Total optical reflectance at the He−Ne wavelength, as a function of graphene thickness. Black and red lines are for the Si and the quartz substrates, respectively.

The decrease of adsorbed molecule Raman intensity with increasing thickness is an intrinsic property of graphene; it occurs in our calculation in the absence of a back mirror(result not shown). The very weak molecular Raman intensity for thick graphene is similar to that observed on reflective flat metals, as originally modeled by Greenler and Slager.[23] The Fresnel equations imply there is a 180° phase shift for reflected light at normal incidence on a highly reflective mirror. Thus a node in the net laser intensity occurs at the adsorbed species on such a metal surface. Also, Raman scattering dipoles oriented in the plane of the surface are diminished by their image dipoles in the metal. Our I_3^- and I_5^- species, and the intercalated anionic bromine, presumably have Raman scattering dipoles in the plane.

Bromine Intercalation. The Raman intensities of interior Br_2 intercalated layers in Figure 2 should behave similarly to the Raman intensities of interior graphene layers. The intercalated layer is a dense molecular monolayer, and as a first approximation we could assume it has similar thickness and index of refraction as a graphene layer. For electromagnetic calculation purposes, the interior laser intensity and the Raman collection efficiency would be the same in an (4L) graphene with an interior intercalated Br_2 layer as in an (5L) graphene without intercalation, for example, with this approximation. This model suggests that the interca-

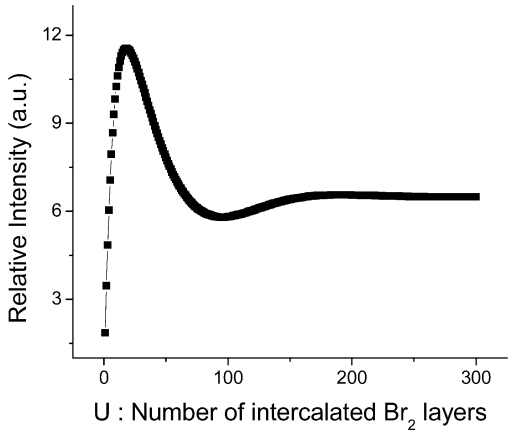

Figure 7. Calculated relative Raman intensity of intercalated Br_2 layers *versus* number of intercalated Br_2 layers. $U = 1$ corresponds to 4L of graphene with one intercalated layer. $U = 2$ corresponds to 6L of graphene with two intercalated layers, and so on. Relative Raman intensity ratio between 1L to 300L intercalated Br_2 is 3.477.

lated layer Raman signal should be enhanced for small *N* as compared with the bulk GIC, in the same way that the G mode Raman signal itself is enhanced for small *N* as compared with bulk graphite.

In the stage two Br_2 GIC, the basic repeating unit is two graphene layers plus a bromine layer, with a total thickness of 1.04 nm. We carried out a Fresnel calculation with an increasing number *U* of intercalated Br_2 repeating units (Supporting Information); in analogy to the G mode calculation for increasing numbers of single graphene layers in Figure 4. The measured optical reflectively of the GIC at the He−Ne laser wavelength is near 0.2, about two-thirds of the pure graphite reflectivity.[24] A lowered reflectivity implies that the GIC effective optical index is lower than that of graphite. While the actual GIC complex index has not been measured, we estimate the index must be near (1.6 −1.3i) to give this reflectivity in an optically absorbing GIC sample. In Figure 7 we plot the bromine Raman collection efficiency as a function of intercalated Br_2 layers *U* using this index. There is agreement within a factor of two with the observed factor of six intensity decrease of one intercalate layer *versus* the bulk GIC.

DISCUSSION

Iodine Adsorption. We can determine the I_3^- and I_5^- combined surface density (per cm^{-2}) on graphene from our understanding of the graphene hole doping. For low *N* we detect the anion Raman signal from both the top and bottom surfaces of graphene. The measured 1L graphene G band frequency is 1608.8 cm^{-1} corresponding to a hole density of $2.6 \times 10^{+13}$ cm^{-2}. This value is interpolated from the electrostatic doping experiment using a field effect device.[25] If we assume that the number of doped holes equals the number of surface iodine anions and that iodine anion surface density on top and bottom surfaces is half the hole density, then the ion surface densities on the top and the bottom of 1L are about $1.3 \times 10^{+13}$ cm^{-2}. For comparison, the graphene carbon atom density is $3.8 \times 10^{15}/cm^2$. We have only about 1 anion per adsorbed layer for every 300 graphene C atoms. If we roughly estimate the iodine anion monolayer coverage to be similar to the intercalated bromine coverage in the stage two GIC C_8Br_2, $4.75 \times 10^{14}/cm^2$, then the observed anion coverage is low, about 3%. Nevertheless, the iodine anion spectra are intense compared to the 1L graphene G spectra, with an integrated intensity ratio of iodine anion to graphene G peak of about 120.

In general Raman scattering is too weak to yield a signal from a monolayer sample without some form of electronic or electromagnetic resonance enhancement, although with extreme sensitivity, monolayer spectra can be observed.[26] We do not observe the Raman scattering of adsorbed neutral I_2, which is essentially transparent at the laser wavelength, or of the underlying 290 nm thick transparent SiO_2 layer. The iodine anions show an intense intramolecular resonance Raman effect due to irradiation into an excited electronic state. Such electronic resonance is common in molecules and has been carefully quantitatively analyzed,[27] including broadening of the resonant state. Enhancement can reach four or five orders of magnitude in intensity.

In comparison, the monolayer graphene G peak is much weaker than the anion peaks and thus shows only a modest resonance Raman effect, despite the fact that graphene absorbs at the laser irradiation wavelength. This absence of strong electronic resonance is often observed in any extended periodic system when excitation directly creates very short-lived "hot" free electrons and holes, rather than a long-lived bound resonant intermediate state.

The experimental adsorbed anion Raman signal decreases continuously with increasing *N* except from 1L to 2L. In Figure 1 the 4L iodine anion signal is about 70% of the 1L signal; this ratio is similar to the calculated decrease in Raman detection sensitivity of 86% in Figure 5 if we sum contributions from both anion layers. Thus for small *N* it seems that the surface concentration of anions is not a large function of graphene thickness. For large *N* the laser light does not penetrate through the graphene, and we only detect anion Raman signals from the top surface. The calculated signal ratio between $N = 1$ and thick graphene should then be 55; we actually observe 30. This comparison assumes the surface density of iodine anions on top of $N = 1$ graphene is the same as on bulk graphite.

It should be noted that the Raman intensity of adsorbed iodine on 2L is slightly larger than on 1L Raman intensity. It is reported that the amount of Li ion adsorbed on 1L graphene is reduced due to repulsion forces on both sides of graphene layers, while the interaction of Li ion with few layer graphene seems to resemble that of graphene.[28] We can similarly argue that the concentration of iodine anions adsorbed on single

layer graphene will be reduced due to repulsion forces, compared with 2L graphene. Repulsion should be negligible for thicker graphenes.

The calculated and observed values differ by a factor of two. Our model does not consider the change in index of refraction due to the adsorbed layers. We also do not consider non-normal angles of incidence despite our experimental use of objective numerical aperture of 0.6, where the light is focused at an angle of 37°, although a preliminary calculation of the graphene G peak intensity that includes numerical aperture effects produces nearly the same result.[21] In addition, our objective has a depth of field of at least 1 μm, so the beam should remain focused through our system. Finally, the surface density of anions may be somewhat larger on bulk graphite, as compared with 1L graphene, because on graphite several near surface layers are doped by charge transfer. But clearly the major effect in the anion Raman spectra on 1L graphene compared to graphite is the large reflection interference effect we calculate.

Our optical interference calculation predicts that Raman detection sensitivity for adsorbed species decreases for increasing N and that bulk graphite is a poor Raman substrate. We see essentially this behavior for adsorbed iodine anions. A similar decreasing Raman signal with increasing N was observed by Ling *et al*. for several adsorbed dye molecules.[29] We assign their observed decreasing signal to the same interference mechanism that governs the iodine anion intensities.

Xie *et al*. report that 1L graphene is an excellent substrate for observation of resonance Raman from adsorbed R6G dye molecules, principally because it strongly quenches R6G luminescence that otherwise would overwhelm resonance Raman scattering.[30] Their R6G Raman spectra are very strong on graphene; the actual coverage was not measured. In our present experiment, we see intense iodine anion Raman spectra at near 3% coverage on graphene. Highly luminescent quantum dots adsorbed on 1L graphene show a factor of 70 luminescence quenching, at a 3.5 nm spacing Z between the dot center and the graphene plane, in quantitative agreement with dipole−dipole energy transfer theory.[31] The quenching rate theoretically increases as Z^{-4} closer to the surface;[32] a simple calculation based upon this theory yields a quenching factor of about 10^{6+} for a typical molecular adsorption at $Z =$ 0.2 nm. It is remarkable that 1L graphene, which is about 98% transparent to visible light, can quench luminescence so efficiently. Strong luminescence quenching is useful in graphene processing applications.[33,34]

In SERS involving Ag and Au particles, two separate effects can occur. By far the most important is electromagnetic field enhancement due to the local fields of scattering dipoles induced in the particles. In agreement with Xie *et al*.,[30] we find no electromagnetic field enhancement on graphene; we calculate a laser intensity enhancement of only 1.3 on the surface of 1L graphene. If for no other reason, this is expected, as the plasmon of any macroscopically flat surface does not couple to far field radiation.

A second and weaker "chemical" SERS effect is an effective change in the adsorbate Raman cross section due to mixing of the surface and absorbate wavefunctions, resulting from charge transfer. Ling *et al*. suggest that such a "chemical" effect can occur for dye molecules on graphene. Actually, the fundamental optics are quite different on graphene and in the aggregated Ag particle systems where very strong SERS occurs: in aggregated Ag the laser field is perpendicular to the local metal surface at positions of high Raman scattering,[3] and in graphene the field is parallel. In the electrostatic approximation, the parallel laser E field has the same magnitude both just above the graphene surface, and in the first graphene layer. That is, graphene does not screen the incident laser E field. This is the basic reason that the calculated behavior of the G Raman band in the first graphene layer (Figure 4) is very similar to that of adsorbed species Raman bands (Figure 5). In contrast, the perpendicular laser E field in SERS is screened by the metal: the laser E field is discontinuous across the surface.

The graphene work function is about 4.5 eV. In molecular language, 4.5 eV is both the graphene electron affinity and the ionization potential; this is an usually high electron affinity and an unusually low ionization potential. These values facilitate the formation of weakly bound charge-transfer complexes with adsorbed species; such molecular complexes have been studied for decades.[35] Indeed, such charge transfer is the reason that halogens dope graphene. Charge-transfer complexes necessarily have a excited charge-transfer electronic transition.[36] Laser irradiation into the charge-transfer transition can create a "chemical" SERS effect; this occurs for molecules adsorbed on Ag.[37] This "chemical" SERS resonance mechanism can increase the Raman intensity of adsorbates initially transparent at the laser wavelength. There should not be much effect on dyes already having an intense intramolecular electronic absorption and resonance at the laser wavelength.

Actually, in molecular resonance Raman theory the Raman intensity decreases strongly with increasing broadening of the resonant excited state.[27] If we compare the Raman cross sections of a species in solution *versus* the same dry species on the graphene surface, then the cross sections surely will be different. Solvent broadening is absent on the surface, however the strong energy transfer quenching of the excited dye lifetime on graphene (from nano- to femtosecond time scales) will create a new large homogeneous broadening of the resonant intermediate excited state. In addition, the local polarizability is higher on the graphene surface than on quartz, or in most solvents. A higher lo-

cal polarizability will tend to shift the adsorbate excited electronic absorption spectra to a lower energy. This shift will change the degree of intramolecular resonance with the laser wavelength, and thus the adsorbate Raman cross section will be different.

We do not see the Raman scattering of weakly adsorbed neutral Br_2 or I_2, with vibrational frequency close to the gas-phase value on graphene; this is expected as these neutral halogens are essentially transparent at the laser wavelength with no electronic resonance. Thus, for adsorbed iodine anion species, the large Raman signal comes from resonance enhancement of the anion intramolecular electronic transition, while the multiple reflection interference calculation explains the Raman signal evolution as a function of graphene thickness.

Bromine Intercalation. There is significant charge transfer from both adsorbed and intercalated Br_2 layers in 1−4L graphenes. We observed[2] that the doping of 2L graphene with adsorbed Br_2 layers on the top and the bottom produces a shift of the graphene G band to 1612 cm^{-1}. There is no intercalated layer for 2L graphene. The same G band frequency is observed in the stage two bulk GIC where doping results only from intercalated Br_2 layers. In the bulk case, one intercalated bromine layer dopes two graphene layers, while in the 2L case, one adsorbed bromine layer dopes one graphene layer. Thus the effective planar electron density in the adsorbed bromine layer is one-half the density in the intercalated layer. In the case of 4L graphene where there is one intercalated layer and two adsorbed layers, this same analysis is valid. Two conclusions can be drawn: (1) equilibrium charge transfer in the ground electronic state, from graphene to bromine, is less efficient for adsorbed bromine layers, and (2) equilibrium charge transfer to an intercalated layer is not sensitive to the total number of graphene layers in the sample.

An extended X-ray absorption fine structure (EXAFS) study of the bulk GIC shows a 16% fractional charge transfer: the density (per cm^{-2}) of transferred electrons is 12% of the $4.8 \times 10^{13}/cm^2$ planar density of Br_2 molecules in the intercalated layer. This significant charge transfer completely changes the graphene electronic properties; Br_2 intercalated graphite shows a "supermetallic" in-plane DC conductivity higher than that of Cu metal.[38] Density functional theory (DFT) calculations show the GIC Fermi level is delocalized onto the Br_2 p orbitals.[39] The intercalated layer is crystalline and shows a first-order phase transition at 373 K.[7] Theory suggests intercalated Br_3^- may form.[40] Possibly we observe intercalated anionic Br_3^- in the Raman scattering, in analogy to I_3^- for iodine. The identity of the bromine species observed in Raman remains unsettled.

We see bromine Raman scattering from the intercalated layer but not from the adsorbed layer. Does this reflect a "chemical" SERS effect with bromine Raman intensity created by excitation into a charge-transfer electronic transition between layers? Even if a charge-transfer electronic transition were present at the laser wavelength, the electronic transition dipole would be perpendicular to the graphene plane and thus would not couple to the laser field at normal incidence. For this reason we do not assign the bromine Raman intensity to a charge-transfer "chemical" SERS effect. Also note that charge-transfer optical transitions have not been identified in the optical spectra of GICs in general.[24] Eklund *et al*. showed there is a very strong electronic resonance Raman effect for the bromine species in the bulk GIC: the bromine Raman intensity increases by two to three orders of magnitude for laser excitation from the red to the blue.[6] Also the bromine Raman spectrum shows a long series of overtones, implying a relatively long-lived resonant intermediate state in Raman theory, which is more typical of intramolecular excited electronic state, such as possibly Br_3^-. In this connection, a comparison between adsorbed I_2 and Br_2 is instructive: The iodine layer shows an intense Raman signal despite exhibiting less net charge transfer with graphene than the bromine layer. This shows the importance of the intramolecular electronic resonance in the observed Raman intensity.

In molecular chemistry, polar molecular electronic states are preferentially stabilized, with respect to nonpolar covalent states, in a polarizable local environment. The percentage of charge transfer in a molecular complex often increases as the solvent dielectric constant increases. Intercalated bromine experiences a higher local dielectric constant than adsorbed bromine in our graphene experiments, and this may be the reason why the percentage of equilibrium charge transfer in the ground electronic state is greater for intercalated bromine than for adsorbed bromine. In addition, as previously mentioned excited electronic states are often stabilized (shifted to lower energy) by a polarizable local dielectric environment. It may also be that the excited intramolecular bromine resonant Raman state in the intercalated layer lies at a lower energy than on the surface. For the He−Ne laser, there would be weak resonance for the intercalated layer and even less resonance for the adsorbed layer. Perhaps for excitation further in the blue both adsorbed and intercalated bromine species would be observed.

In some GICs the graphene G band itself shows a stronger electronic resonance than we observe here. In GICs a graphene π to π^* interband optical absorption edge is created by the Fermi level shift and can be identified in the optical spectra.[24] Laser excitation near this optical edge typically yields a strong G band Raman electronic Raman resonance.[41] In the stage two bromine GIC, however, our 1.93 eV He−Ne laser is far above the measured interband edge at 1.1 eV.[24]

The large Raman signal from intercalated bromine is attributed to resonance enhancement of an intramolecular electronic transition. Also, recall that the multiple reflection interference calculation gave a reasonable result for the ratio of the bromine Raman signal for

4L graphene to the bulk. Thus, the magnitude of the Raman signal is attributed to intramolecular electronic resonance enhancement, and the evolution with graphene thickness is explained by the electromagnetic interference calculation. This is the same general result as for iodine adsorption.

SUMMARY

Optically transparent single and few layer graphenes are excellent substrates for molecular adsorbate Raman scattering. Multiple reflection Fresnel calculations show a strongly decreasing Raman sensitivity for thicker graphenes, while bulk graphite is a poor substrate. Molecular species showing intramolecular electronic resonance can be detected at a small fraction of a monolayer coverage on single layer graphene. This sensitivity occurs because graphene efficiently quenches interfering molecular excited state luminescence, rather than significantly intensifying the electromagnetic fields or creating a "chemical" surface enhanced Raman spectroscopy (SERS) effect.

METHODS

Our experimental methods have been previously described.[2] In brief, graphene pieces were deposited by mechanical exfoliation in air onto Si wafer chips with a 290 nm thick surface SiO_2. In one experiment graphene pieces of different thickness are present at different places on the substrate. The graphene pieces were initially characterized by Raman at 514 nm to determine thickness. Halogen exposure was performed using a conventional two temperature zone apparatus;[1] measurements were made at 23 °C with all pieces in equilibrium with gaseous halogen. We perform confocal backscattering Raman with a *ca.* 4 μm^2 spot size using about 3.2 mW of 633 nm He−Ne laser irradiation. The halogen-induced changes in the graphene G Raman spectra were described and analyzed previously.[2]

Acknowledgment. We thank M. Steigerwald, T. Heinz, and Zhang Jin (Beijing) for productive discussions. We also thank S. Jockusch and N.J. Turro for constructive experimental advice and for access to vacuum apparatus. This work was funded by the Department of Energy under grant DE-FG02-98ER14861(LEB), by the AFORSR MURI (P.K.). We acknowledge financial support from the Nanoscale Science and Engineering Initiative of the National Science Foundation under NSF award no. CHE-06-41523 and by the New York State Office of Science, Technology, and Academic Research (NYSTAR).

Supporting Information Available: Equations for the graphene G-peak and bromine peak Raman signal as a function of graphene thickness and a table of fitting paramters are present. This material is available free of charge *via* the Internet at http://pubs.acs.org.

REFERENCES AND NOTES

1. Dresselhaus, M. S.; Dresselhaus, G. Intercalation Compounds of Graphite. *Adv. Phys.* **2002**, *51*, 1–186.
2. Jung, N.; Kim, N.; Jockusch, S.; Turro, N. J.; Kim, P.; Brus, L. Charge Transfer Chemical Doping of Few Layer Graphenes: Charge Distribution and Band Gap Formation. *Nano Lett.* **2009**, *9*, 4133–4137.
3. Brus, L. Noble Metal Nanocrystals: Plasmon Electron Transfer Photochemistry and Single-Molecule Raman Spectroscopy. *Acc. Chem. Res.* **2008**, *41*, 1742–1749.
4. Nemanich, R. J.; Tsai, C. C.; Connell, G. A. N. Interference-Enhanced Raman-Scattering of Very Thin Titanium and Titanium-Oxide Films. *Phys. Rev. Lett.* **1980**, *44*, 273–276.
5. Sasa, T.; Takahash, Y; Mukaibo, T. Crystal Structure of Graphite Bromine Lamellar Compounds. *Carbon* **1971**, *9*, 407–416.
6. Eklund, P. C.; Kambe, N.; Dresselhaus, G.; Dresselhaus, M. S. In-Plane Intercalate Lattice Modes in Graphite-Bromine Using Raman-Spectroscopy. *Phys. Rev. B: Solid State* **1978**, *18*, 7069–7079.
7. Erbil, A.; Dresselhaus, G.; Dresselhaus, M. S. Raman-Scattering as a Probe of Structural Phase-Transitions in the Intercalated Graphite-Bromine System. *Phys. Rev. B: Condens. Matter Mater. Phys.* **1982**, *25*, 5451–5460.
8. Song, J. J.; Chung, D. D. L.; Eklund, P. C.; Dresselhaus, M. S. Raman-Scattering in Graphite Intercalation Compounds. *Solid State Commun.* **1976**, *20*, 1111–1115.
9. Hooley, J. G. Physical-Chemistry and Mechanism of Intercalation in Graphite. *Mater. Sci. Eng.* **1977**, *31*, 17–24.
10. do Nascimento, G. M.; Hou, T.; Kim, Y. A.; Muramatsu, H.; Hayashi, T.; Endo, M.; Akuzawa, N.; Dresselhaus, M. S. Comparison of the Resonance Raman Behavior of Double-Walled Carbon Nanotubes Doped with Bromine or Iodine Vapors. *J. Phys. Chem. C* **2009**, *113*, 3934–3938.
11. Zhou, W. Y.; Xie, S. S.; Sun, L. F.; Tang, D. S.; Li, Y. B.; Liu, Z. Q.; Ci, L. J.; Zou, X. P.; Wang, G.; Tan, P. Raman Scattering and Thermogravimetric Analysis of Iodine-Doped Multiwall Carbon Nanotubes. *Appl. Phys. Lett.* **2002**, *80*, 2553–2555.
12. Cambedouzou, J.; Sauvajol, J. L.; Rahmani, A.; Flahaut, E.; Peigney, A.; Laurent, C. Raman Spectroscopy of Iodine-Doped Double-Walled Carbon Nanotubes. *Phys. Rev. B: Condens. Matter Mater. Phys.* **2004**, *69*, 235422.
13. Limonov, M. F.; Kitaev, Y. E.; Chugreev, A. V.; Smirnov, V. P.; Grushko, Y. S.; Kolesnik, S. G.; Kolesnik, S. N. Phonons and Electron-Phonon Interaction in Halogen-Fullerene Compounds. *Phys. Rev. B: Condens. Matter Mater. Phys.* **1998**, *57*, 7586–7594.
14. Brinkmann, M.; Videva, V. S.; Bieber, A.; Andre, J. J.; Turek, P.; Zuppiroli, L.; Bugnon, P.; Schaer, M.; Nuesch, F.; Humphry-Baker, R. Electronic and Structural Evidences for Charge Transfer and Localization in Iodine-Doped Pentacene. *J. Phys. Chem. A* **2004**, *108*, 8170–8179.
15. Cazayous, M.; Sacuto, A.; Horowitz, G.; Lang, P.; Zimmers, A.; Lobo, R. Iodine Insertion in Pentacene Thin Films Investigated by Infrared and Raman Spectroscopy. *Phys. Rev. B: Condens. Matter Mater. Phys.* **2004**, *70*, 081309.
16. Marikhin, V. A.; Novak, I. I.; Kulik, V. B.; Myasnikova, L. P.; Radovanova, E. I.; Belov, G. P. Resonant Raman Spectroscopy of Ethylene-Acetylene Copolymers Doped with Iodine. *Phys. Solid State* **2002**, *44*, 1188–1195.
17. Wang, D. K.; Tsukamoto, J.; Takahashi, A.; Muraki, N.; Katagiri, G. Polarized Resonance Raman-Scattering of Iodine-Doped Polyacetylene with High-Conductivity. *Synth. Met.* **1994**, *65*, 117–122.
18. Sharp, S. B.; Gellene, G. I. Ab Initio Calculations of the Ground Electronic States of Polyiodide Anions. *J. Phys. Chem A* **1997**, *101*, 2192–2197.
19. Connell, G. A. N.; Nemanich, R. J.; Tsai, C. C. Interference Enhanced Raman-Scattering from Very Thin Absorbing Films. *Appl. Phys. Lett.* **1980**, *36*, 31–33.
20. Palik, E. D. *Handbook of Optical Constants of Solids*; Academic Press: San Diego, CA, 1998.
21. Yoon, D.; Moon, H.; Son, Y. W.; Choi, J. S.; Park, B. H.; Cha, Y. H.; Kim, Y. D.; Cheong, H. Interference Effect on Raman Spectrum of Graphene on Sio2/Si. *Phys. Rev. B: Condens. Matter Mater. Phys.* **2009**, *80*, 125422.
22. Wang, Y. Y.; Ni, Z. H.; Shen, Z. X.; Wang, H. M.; Wu, Y. H. Interference Enhancement of Raman Signal of Graphene. *Appl. Phys. Lett.* **2008**, *92*, 043121.

23. Greenler, R. G.; Slager, T. L. Method for Obtaining Raman-Spectrum of a Thin-Film on a Metal Surface. *Spectrochim. Acta, Part A* **1973**, *A 29*, 193–201.
24. Blinowski, J.; Hau, N. H.; Rigaux, C.; Vieren, J. P.; Letoullec, R.; Furdin, G.; Herold, A.; Melin, J. Band-Structure Model and Dynamical Dielectric Function in Lowest Stages of Graphite Acceptor Compounds. *J. Phys. (Paris)* **1980**, *41*, 47–58.
25. Das, A.; Pisana, S.; Chakraborty, B.; Piscanec, S.; Saha, S. K.; Waghmare, U. V.; Novoselov, K. S.; Krishnamurthy, H. R.; Geim, A. K.; Ferrari, A. C.; Sood, A. K. Monitoring Dopants by Raman Scattering in an Electrochemically Top-Gated Graphene Transistor. *Nat. Nanotechnol.* **2008**, *3*, 210–215.
26. Kambhampati, P.; Song, O. K.; Campion, A. Probing Photoinduced Charge Transfer at Atomically Smooth Metal Surfaces Using Surface Enhanced Raman Scattering. *Phys. Status Solidi A* **1999**, *175*, 233–239.
27. Myers, A. B. 'Time-Dependent' Resonance Raman Theory. *J. Raman Spectrosc.* **1997**, *28*, 389–401.
28. Pollak, E.; Geng, B. S.; Jeon, K. J.; Lucas, I. T.; Richardson, T. J.; Wang, F.; Kostecki, R. The Interaction of Li+ with Single-Layer and Few-Layer Graphene. *Nano Lett.* **2010**, *10*, 3386–3388.
29. Ling, X.; Xie, L. M.; Fang, Y.; Xu, H.; Zhang, H. L.; Kong, J.; Dresselhaus, M. S.; Zhang, J.; Liu, Z. F. Can Graphene Be Used as a Substrate for Raman Enhancement. *Nano Lett.* **2010**, *10*, 553–561.
30. Xie, L. M.; Ling, X.; Fang, Y.; Zhang, J.; Liu, Z. F. Graphene as a Substrate to Suppress Fluorescence in Resonance Raman Spectroscopy. *J. Am. Chem. Soc.* **2009**, *131*, 9890–9891.
31. Chen, Z.; Berciaud, S.; Nuckolls, C.; Heinz, T. F.; Brus, L. E. Energy Transfer from Individual Semiconductor Nanocrystals to Graphene. *ACS Nano* **2010**, *4*, 2964–2968.
32. Swathi, R. S.; Sebastian, K. L. Long Range Resonance Energy Transfer from a Dye Molecule to Graphene Has (Distance)(−4) Dependence. *J. Chem. Phys.* **2009**, *130*, 086101.
33. Kim, J.; Cote, L. J.; Kim, F.; Huang, J. X. Visualizing Graphene Based Sheets by Fluorescence Quenching Microscopy. *J. Am. Chem. Soc.* **2010**, *132*, 260–267.
34. Sagar, A.; Kern, K.; Balasubramanian, K. Marker-Free on-the-Fly Fabrication of Graphene Devices Based on Fluorescence Quenching. *Nanotechnology* **2010**, *21*, 015303.
35. Bender, C. J. Theoretical-Models of Charge-Transfer Complexes. *Chem. Soc. Rev.* **1986**, *15*, 475–502.
36. Abdou, M. S. A.; Orfino, F. P.; Xie, Z. W.; Deen, M. J.; Holdcroft, S. Reversible Charge-Transfer Complexes between Molecular-Oxygen and Poly(3-Alkylthiophene)S. *Adv. Mater.* **1994**, *6*, 838–841.
37. Lombardi, J. R.; Birke, R. L.; Lu, T. H.; Xu, J. Charge-Transfer Theory of Surface Enhanced Raman-Spectroscopy - Herzberg-Teller Contributions. *J. Chem. Phys.* **1986**, *84*, 4174–4180.
38. Tongay, S.; Hwang, J.; Tanner, D. B.; Pal, H. K.; Maslov, D.; Hebard, A. F. Supermetallic Conductivity in Bromine-Intercalated Graphite. *Phys. Rev. B: Condens. Matter Mater. Phys.* **2010**, *81*, 035427.
39. Rudenko, A. N.; Keil, F. J.; Katsnelson, M. I.; Lichtenstein, A. I. Adsorption of Diatomic Halogen Molecules on Graphene: A Van Der Waals Density Functional Study. *Phys. Rev. B: Condens. Matter Mater. Phys.* **2010**, *82*, 035427.
40. Higai, S.; Mizuno, S.; Suzuki, S.; Nakao, K. Electronic Structure and Charge Transfer Mechanism of Bromine-Graphite Intercalation Compound. *Mol. Cryst. Liq. Cryst. Sci. Technol., Sect. A* **1998**, *310*, 267–272.
41. Eklund, P. C.; Mahan, G. D.; Spolar, J. G.; Arakawa, E. T.; Zhang, J. M.; Hoffman, D. M. Resonant Interband Raman-Scattering in Metals and Semimetals. *Solid State Commun.* **1986**, *57*, 567–570.